

IDSCAN  
LVL2 Tracking for the ATLAS Trigger  
1st Year Transfer Report

Janice Drohan  
University College London

June 20, 2003



### Abstract

IDSCAN is a Track Reconstruction algorithm for the ATLAS Second Level Trigger. It currently runs in the offline ATHENA Software environment and in the High Level Trigger Event Selection Software (HLTSSW). Efficiencies are calculated with respect to the xKalman full reconstruction package, with cuts applied to the  $\eta$ ,  $\phi$ ,  $z_0$  and  $P_T$  of the track from the true values. For 30GeV single electron events at high luminosity the ATHENA version has a current efficiency of 93.3%, compared to 83.3% for the HLTSSW version. A description of the current analysis for the channel  $t\bar{t}H, H \rightarrow b\bar{b}$  is presented, along with an assessment of where possible improvements could be made.



# Contents

<b>Contents</b>	<b>iii</b>
<b>1 Introduction</b>	<b>1</b>
1.1 ATLAS	1
1.2 High-Level Trigger (HLT)	2
1.2.1 Level 2 System	2
1.2.2 Event Filter	2
1.2.3 Event Selection Software	3
1.3 IDSCAN	4
1.3.1 Algorithm	4
1.3.2 Offline Version - ATHENA Environment	5
1.3.3 Online Version - High-Level Trigger Environment	5
<b>2 IDSCAN Validation</b>	<b>7</b>
<b>3 Future Plans</b>	<b>13</b>
3.1 IDSCAN	13
3.2 Atlantis	13
3.3 Associated Higgs Production: $t\bar{t}H$	13
<b>Bibliography</b>	<b>17</b>



# 1. Introduction

IDSCAN is an Inner Detector Track Reconstruction algorithm for the ATLAS Second Level Trigger. This section introduces the physics objectives of the ATLAS experiment and the triggering system employed. This is followed by a description of the algorithm, the concepts it is based on and the environments in which it is run. The IDSCAN Validation chapter describes the work done to assess the performance of the algorithm in the run up to the High-Level Trigger TDR, due to be published in June, particularly for high  $P_T$  electrons. Triggering on such electrons is very important for the channel  $t\bar{t}H$ ,  $H \rightarrow b\bar{b}$ , which is estimated to provide half the significance for a discovery of a low mass Standard Model Higgs Boson. This channel shall be investigated during the second year of my PhD, specifically the largest background  $t\bar{t}jj$ . The final section summarises the TDR analysis and improvements made in recent years.

## 1.1 ATLAS

The LHC will collide protons with a center of mass energy of 14TeV and design luminosity of  $10^{34} \text{cm}^{-2} \text{s}^{-1}$ , offering a large range of physics opportunities. For the ATLAS detector the major focus of interest is to understand the mechanism of electroweak symmetry breaking, by searching for one or more Higgs bosons. Other important goals are searches for heavy W- and Z-like objects, super-symmetric particles, the compositeness of the fundamental fermions, investigation of CP violation in B-decays and detailed studies of the top quark [ATL94].

Event selection at LHC faces a huge range in cross-section values for various processes. The total proton-proton inelastic cross section is estimated to be 80mb, compared to a rate of 20pb for the production for a Standard Model Higgs Boson with mass 120GeV. The selection strategy has to ensure that rare signals will not be missed whilst providing an efficient rejection of high rate backgrounds. The LHC bunch-crossing rate is 40MHz, one every 25ns, and at design luminosity there are about 23 interactions per bunch crossing. The ATLAS triggering system has to reduce this rate to match the event storage, limited to approximately 200Hz by restrictions in the offline computing power and storage capabilities (each event is about 2MByte in size to store).

Due to these constraints, the ATLAS trigger and data-acquisition system is based on three levels of on-line event selection, shown in Figure 1.1. Each trigger level refines the decisions made at the previous level and applies additional selection criteria.

At the first level (LVL1) purpose built processors act on reduced granularity data from the calorimeters and muon trigger chambers. A decision by the LVL1 Trigger has to be made within  $2\mu\text{s}$ . This is carried out by a system of custom-electronics with hard-wired algorithms. At the second level full-granularity, full-precision data is available from all of the detectors, but only in Regions of Interest (RoI) identified by LVL1. LVL2 must reduce the rate to 1kHz with a latency of 1ms. At the third level, the Event Filter has access to the full event data as well as calibration and alignment information. This is used to make the final decision before the event is recorded, with a target latency of 1s.

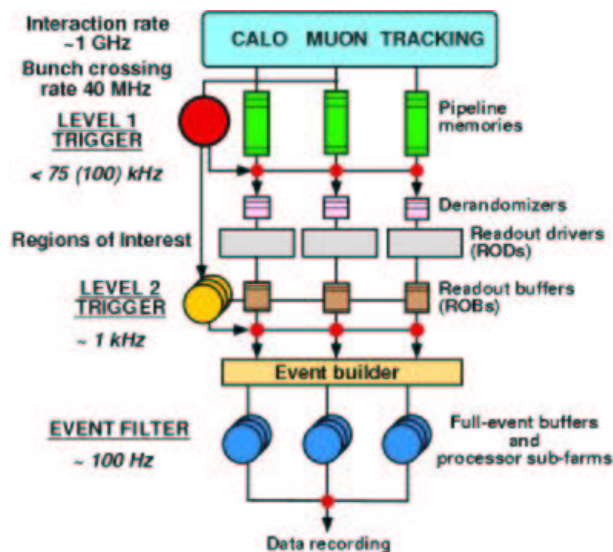


Figure 1.1: ATLAS Trigger and DAQ System

## 1.2 High-Level Trigger (HLT)

The High-Level Trigger is based on logically separate LVL2 and Event Filter selection stages, enabling maximum flexibility in distributing the selection process between the two levels. This flexibility allows for changes such as luminosity, detector knowledge and background conditions. The HLT comprises of three main parts, the LVL2 system, the Event Filter system and the Event Selection Software (ESS) [ATL03a, ATL03b].

### 1.2.1 Level 2 System

The LVL2 system is composed of the RoI Builder, LVL2 Supervisor, LVL2 Processors, the Read Out System (ROS) and the pseudo-ROS (pROS). The RoI builder assembles fragments of information from different parts of the LVL1 trigger and transmits the combined record to the LVL2 supervisor. The supervisor then selects a LVL2 Processor for the event, sends the LVL1 information to it and waits for a decision. The LVL2 Processing Unit runs the Event Selection Software requesting relevant event data as required from the ROS. A decision is then returned to the supervisor. For events that pass the LVL2 stage, the result is sent to the pROS where the event is built and sent on to the Event Filter.

Processing is performed by a single application consisting of three components, the Level 2 Processing Unit (L2PU), the PESA<sup>1</sup> Steering Controller and the ESS. The L2PU handles the data flow with other parts of the HLT and the PESA Steering Controller runs inside the L2PU providing the required environment and services needed by the ESS.

### 1.2.2 Event Filter

The Event Filter (EF) makes use of the offline software framework ATHENA and the ESS to execute filtering algorithms based directly on offline reconstruction. It

<sup>1</sup>Physics Event Selection Architecture



has two main parts, the Event Handler (EH) and the EF Supervisor. The EH is in charge of the data flow between the main Data Acquisition system and the EF. It also deals with the different steps of event selection. The Supervisor is in charge of control operations and monitoring.

### 1.2.3 Event Selection Software

The ESS is responsible for event selection and classification. It constructs abstract objects (Trigger Elements (TE)) representing candidate electrons, muons, jets etc from the event data using a particular set of HLT algorithms and applying appropriate cuts. The event is selected if the reconstructed objects satisfy at least one of the physics signatures given in a trigger menu. Figure 1.1 shows examples of various selection criteria and the physics processes these cover. Selection criteria are designed to meet signal efficiency and rate reduction targets for the trigger.

Selection Signature	Examples of physics coverage
e25i	$W \rightarrow l\nu, Z \rightarrow ll, \text{top production}, H \rightarrow WW^{(*)}/ZZ^{(*)}, W', z'$
2e15i	$Z \rightarrow ll, H \rightarrow WW^{(*)}/ZZ^{(*)}$
$\mu$ 20i	$W \rightarrow l\nu, Z \rightarrow ll, \text{top production}, H \rightarrow WW^{(*)}/ZZ^{(*)}, W', z'$
2 $\mu$ 10	$Z \rightarrow ll, H \rightarrow WW^{(*)}/ZZ^{(*)}$
$\gamma$ 60i	direct photon production, $H \rightarrow \gamma\gamma$
2 $\gamma$ 20i	$H \rightarrow \gamma\gamma$
j400	QCD, SUSY, new resonances
2j350	QCD, SUSY, new resonances
3j165	QCD, SUSY
4j110	QCD, SUSY
$\tau$ 60	charged Higgs
$\mu$ 10+e15i	$H \rightarrow WW^{(*)}/ZZ^{(*)}, SUSY$
$\tau$ 35+xE45	$qqH(\tau\tau), W \rightarrow \tau\nu, Z \rightarrow \tau\tau, SUSY$ at large $\tan\beta$
j70+xE70	SUSY
xE200	new phenomena
E1000	new phenomena
jE1000	new phenomena
2 $\mu$ 6 + $\mu^+\mu^-$ +mass cuts	rare B-decays ( $B \rightarrow \mu\mu X$ ) and $B \rightarrow J/\psi(\psi')X$

Table 1.1: Trigger menu, showing inclusive physics triggers. e25i is an isolation electron with  $P_T > 25\text{GeV}$

HLT Algorithms are comprised of the following types:

**Data Preparation** Raw data from the ATLAS detector will be delivered in terms of a bytestream, formatted in a sub-detector dependant manner. This bytestream must be converted into objects which can then be used by reconstruction algorithms. The Event Filter closely follows the offline reconstruction chain where raw data is converted into Raw Data Objects (RDOs), which are then processed to give SCT clusters or calorimeter cells. In LVL2 the data preparation goes from raw data to Reconstruction Input Objects (RIOs) in one step. This is a faster, less precise method chosen due to the constraints on the LVL2 latency.

**Feature Extraction** *Reconstruction algorithms* process features and produce new types of features. *Hypothesis algorithms* validate the physics interpretation implied by the label of a trigger element based on the reconstructed features. An example of this is matching a reconstructed calorimeter cell to a track for an electron object.

In general, two parallel reconstruction algorithms are developed side by side for each aspect of reconstruction. The LVL2 algorithms for the Pixel and SCT sub-detectors are IDSCAN and SiTrack. For the TRT these are TRTxKalman and TRT-LUT. muFast and BMC\_TRIG have been developed for the muon system and T2Calo for the Electromagnetic Calorimeter.

## 1.3 IDSCAN

### 1.3.1 Algorithm

IDSCAN [NK00] is a LVL2 track reconstruction algorithm. It takes space-points from the Pixel and SCT detectors as input, returning track parameters, pointers to the space-points from each track and an error matrix.

An ATLAS event at design luminosity contains approximately 30,000 SCT and Pixel Hits, with around 230 in an electron RoI. To reduce the combinatorics which lead to a long execution time for such events, IDSCAN utilises 2 basic principles:

- There is a significant spread in the  $z$  of the various interactions (at the LHC  $\sigma_z = 6\text{cm}$ ).
- Physics events have on average higher transverse momentum than pile-up

The IDSCAN approach consists of 4 separate steps:

**ZFinder** The ZFinder determines the  $z$ -position of the physics event. The RoI is divided into many small bins in  $\phi$  approximately  $0.2\text{-}0.3^\circ$ . In a given  $\phi$  bin, each pair of hits from different layers are used to calculate a  $z$ -position by linear extrapolation to the beam line <sup>2</sup>. A one dimensional histogram is created and filled with the  $z$ -values calculated for each pair. To reduce loss due to binning effects (tracks on the boundary of bins which would give fewer hit pairs) the hits from a given  $\phi$  bin are also combined with those from the two neighbouring bins. The  $z$ -position of the physics event is taken to be the one corresponding to the  $z$ -histogram bin with the maximum number of entries.

The division of the RoI into small  $\phi$  bins gives naturally more weight to high  $P_T$  tracks which would have more hits contained in a single bin.

IDSCAN was developed in CTRIG, an early version of the trigger software. For 40GeV electrons at design luminosity the ZFinder selects the seven space-points from the electron track out of the two hundred and thirty in the RoI with an efficiency of  $97.5\pm 0.4\%$  and resolution of  $180\pm 5\mu\text{m}$  within the CTRIG framework.

**HitFilter** The HitFilter utilises the property that all tracks of sufficiently high  $P_T$  are contained in a small solid angle in  $(\eta, \phi)$  that starts from the track's initial  $z$ -position. Firstly a two dimensional histogram in  $(\eta, \phi)$  is created. For each bin the number of different layers containing hits is counted and entered into the histogram. Hits from neighbouring bins are clustered into groups to eliminate binning effects and, if there are at least five (out of seven) hits in the bin, the hits are accepted. Not all groups of hits are track candidates as narrow jets would not be split up by this step. At this point of the algorithm sequence, around 95% of hits are rejected

---

<sup>2</sup>Tracks are straight lines in  $\rho$ - $z$  assuming a solenoidal magnetic field.

**Group Cleaner** The Group cleaner has the task of removing remaining noise hits from the groups and creating track candidates. Triplets of hits are combined and five helix parameters calculated. Cuts are made on several of these parameters such as  $P_T$  and  $\frac{d^2z}{d\rho^2}$ , and accepted triplets are placed into a two dimensional histogram in  $\phi_0$  and  $\frac{1}{P_T}$ . If a bin contains enough space-points in different layers (five out of seven) then the hits contained are accepted as a good track candidate.

**Track Fitter** The track candidates are passed to a standard kalman-type fitting package.

### 1.3.2 Offline Version - ATHENA Environment

ATHENA is a control framework for ATLAS software. It provides four main services that algorithms can use; the Event Data Store (also known as Transient Event Store (TES)), the Detector Data Store, a histogram service and a message service. The offline version of IDSCAN runs directly in ATHENA, retrieving Silicon space-points and truth information from the TES. IDSCAN then constructs its own RoI, based on truth information, and accepts only space-points within this Region. IDSCAN is run only once per event.

### 1.3.3 Online Version - High-Level Trigger Environment

ATHENA is also the framework used by the HLT. It is used by the EF to run offline reconstruction algorithms and in the modified form provided by the PESA steering controller for LVL2. The use of ATHENA for the HLT facilitates the development of algorithms, enables the boundary between LVL2 and EF to be studied and enables performance studies for physics analysis.

In the offline environment ESS emulates the full online selection chain using three top level ATHENA algorithms; a LVL1 trigger emulation, one instance of ESS configured to execute LVL2 algorithms seeded by the LVL1 result and a second instance to execute the EF algorithms seeded by the LVL2 result.

A HLT algorithm requests data within a certain region by first feeding the parameters of the region to the RegionSelector. The RegionSelector returns a set of offline identifiers which the algorithm uses to request collections of relevant data objects from the Transient Event Store (TES). If the TES does not contain the data objects it requests them from a RawDataConverter. The offline identifiers are translated into online or Read-Out Buffer (ROB) identifiers which are then used to request data from the data collection system. The raw data returned from the data collection system is in bytestream format. It is converted into data objects and stored in the TES in collections tagged with offline identifiers. The TES then returns the collections of data objects originally requested by the algorithm [Gro03a], shown in Figure 1.2.

In this environment IDSCAN may be executed several times per event, once for each RoI.

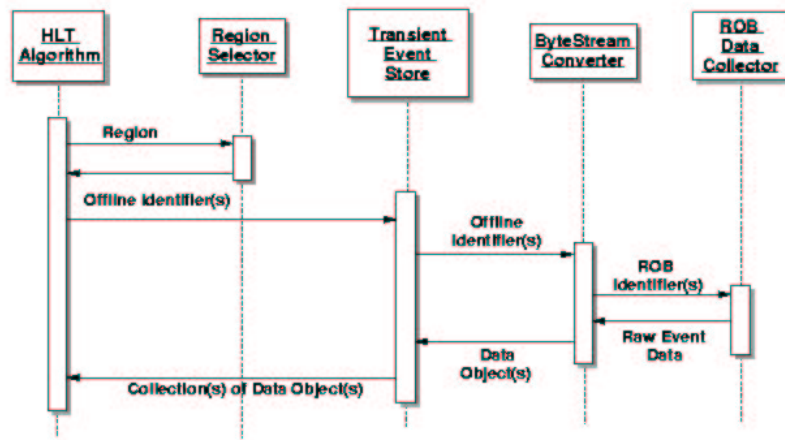


Figure 1.2: HLT algorithm access to raw data information by means of bytestream converters and the TES [Gro03b].

## 2. IDSCAN Validation

The majority of the work carried out this year is related to IDSCAN. The High-Level Trigger Technical Design Report is due to be published on the 30<sup>th</sup> June 2003. Work started in September to integrate IDSCAN into the ATHENA and then into the High Level Trigger environment ready for data production for the TDR.

Initial work included a short study of the ZFinder efficiency in CTRIG for high  $P_T$  electrons (40GeV). The ZFinder  $z_0$  value minus the true value was obtained. For 2000 events taking a cut at 0.2cm yielded an efficiency of 96.8% and tightening this cut to 0.05cm yielded 94.4%. This corresponds to a resolution for  $z_0$  of 175 $\mu$ m.

In the ATHENA framework, IDSCAN has to obtain SCT and Pixel detector information from the ATHENA TES and create its own internal space-points or Hits for use within the algorithm. The internal hits contain only the information from the space-points that are used by IDSCAN. These are  $r$ ,  $\phi$ ,  $z$ , a layer number and an  $\eta$  value. Code was implemented to retrieve the space-points, assign a layer number to the hit according to the internal numbering of IDSCAN and add errors to the hit  $r$ ,  $\phi$ ,  $z$  co-ordinates according to whether they are from the barrel or endcap, SCT or Pixel detectors. The errors are added in the same manner as used in CTRIG.

IDSCAN uses a layer numbering scheme ranging from zero to nineteen. Zero, one and two belong to the Pixel Barrel, three to six to the SCT Barrel, seven to ten belong to the Pixel Endcap and eleven to nineteen the SCT Endcap. The ATHENA space-points contain boolean variables to identify whether they are in the barrel or from the pixel detector and a layer number to identify a specific part of the sub-detector. Using these it is possible to construct a layer numbering scheme as described above.

This method had to be updated for version 6.0.2 of the ATLAS software, where the layer number was removed from the space-points. Now clusters from the space-points class are used to obtain an identifier which contains this information.

The first performance studies of the offline version of IDSCAN were carried out with single muon events with no pile-up. Muon events with  $P_T=3;30;100$ GeV were used. xKalman was run on these events, as well as IDSCAN. This is a full reconstruction package that will be used for the offline analysis, so if xKalman cannot reconstruct a track then these events can be ignored.

Figure 2.1 shows the  $P_T$  distribution from the truth value for a 10GeV Muon. The offset from zero is about 5% of the Muon  $P_T$  and is the same for 3GeV and 100GeV. The large tail that is overestimating the  $P_T$  is also a problem. Figure 2.2 shows the reconstructed  $P_T$  as a function of  $\eta$  and it is clear the tail is from the endcaps. This is a problem that would not have occurred when running the old CTRIG trigger simulation. It is a consequence of the improved detector model DC1. There are a number of changes in DC1, including an improved magnetic field model. This includes the decrease in magnetic field from  $B=2$ T at  $\eta=0$ ,  $B=1$ T at the end of the solenoid, down to  $B=0.4$ T at  $\eta=2.5$ . The Track Fitting routine used by IDSCAN assumes a constant magnetic field. This causes an overestimation in  $P_T$  in the endcaps of the Inner Detector. Here, the tracks are effected less by the magnetic field and hence are straighter indicating a higher  $P_T$ .

After further study into the 5% underestimation, and an event by event comparison of results from the ATHENA and CTRIG versions for electron events (there are no muon data files available), it was concluded that this is a feature of the fitting

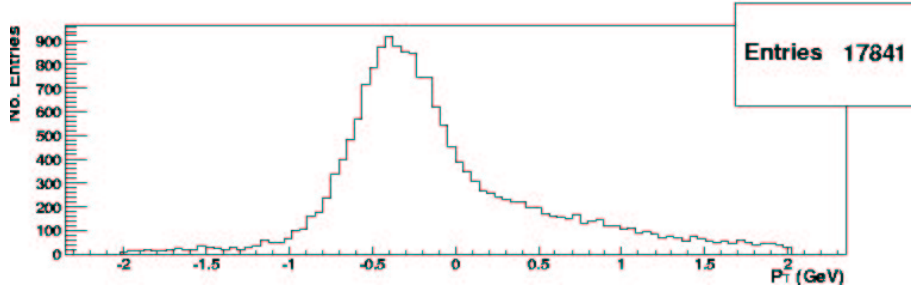


Figure 2.1: Reconstructed track  $P_T$  for 10GeV Muon

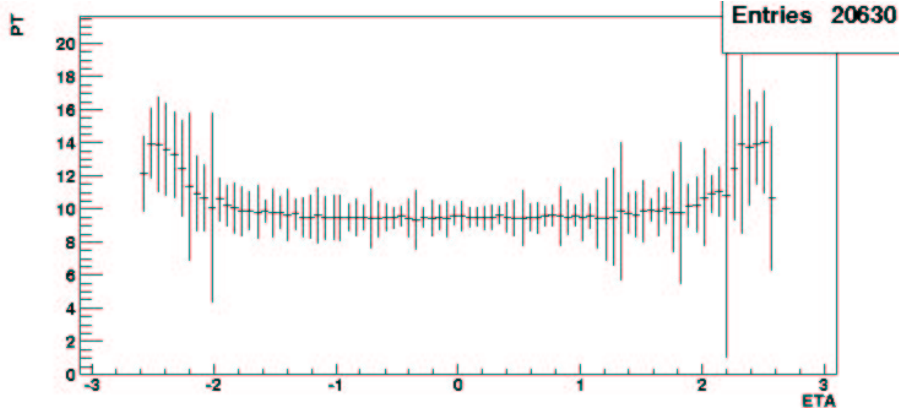


Figure 2.2:  $P_T$  vs  $\eta$  for 10GeV Muon

package. Both of these problems will be dealt with when IDSCAN undergoes a redesign this summer.

For validation of IDSCAN using electrons, datasets with pile-up added for low luminosity (4.6 minimum-bias events added) and high luminosity (23 minimum-bias events added) were available. Due to the increase in the execution times for such events, jobs were submitted to the CERN LXBATCH system and because of instabilities over the long execution times, events were submitted in groups of one hundred for low luminosity and twenty for high luminosity. Analysis of the ZFinder and HitFilter stages were performed separately by including ZFinder information into the output Ntuple and by running IDSCAN using the Monte Carlo truth instead of the ZFinder stage.

For the ZFinder the efficiency is calculated by taking a cut of  $|z_0 - z_{0true}| < 0.5\text{cm}$ .

	Low Luminosity		High Luminosity	
	20GeV	30GeV	20GeV	30GeV
Efficiency (%)	96.9	98.3	89	95.5
Resolution ( $\mu\text{m}$ )	190	170	220	210

Table 2.1: ZFinder efficiencies for the offline IDSCAN version (1000 low luminosity events, 200 high luminosity events)

Compared to the CTRIG ZFinder efficiency of 96.8% and a resolution of  $175\mu\text{m}$  for high luminosity 40GeV Electron events<sup>1</sup>, the results are comparable for low

<sup>1</sup>Here a cut of 0.2 was applied instead of 0.5, this makes little difference.

luminosity, see Table 2.1. However, the high luminosity results are a lot worse than expected. This could be due to the small sample size (only 200 high luminosity events) or the new DC1 detector model. Changes to the model include increased material in the inner detector and the B-layer of the Pixel Detector being positioned at 5.0cm instead of 4.3cm from the beam pipe.

For the HitFilter, validation has been carried out with respect to the xKalman full reconstruction package. Only events where xKalman is able to reconstruct tracks satisfying the following criteria are considered:

- $\Delta r = \sqrt{(\eta - \eta_{true})^2 + (\phi - \phi_{true})^2} < 0.1$
- $Z_0 - Z_{0true} < 0.2$
- $|\frac{P_T - P_{Ttrue}}{P_{Ttrue}}| < 0.5$

IDSCAN and xKalman reconstruct more than one track in most events. A single track is selected from each event using matching to the truth  $\eta$  and  $\phi$  values for the electron candidate.

For events where the xKalman track satisfied the above criteria, the same criteria are applied to the IDSCAN track.

Table 2.2 shows the efficiency for the HitFilter and subsequent stages is around 97%. There is a slight increase in efficiency at high luminosity, this is also present in CTRIG and is due to pile-up adding extra hits to tracks which would have failed the HitFilter stage due to the requirement of five or more hits in different layers. The remaining 3% of events fall into one of three categories; xKalman has reconstructed a very low  $P_T$  track (of order of 1GeV) due to hard bremsstrahlung, the track has a low number of hits from the electron candidate or the track is at very high  $\eta$  ( $\eta > 2$ ).

	Low Luminosity			High Luminosity	
	15GeV	20GeV	30GeV	20GeV	30GeV
IDSCAN Events	819	800	810	159	160
xKalman Events	847	829	834	162	165
Efficiency	96.5%	96.5%	97.1%	98.1%	97.9%

Table 2.2: HitFilter, Group Cleaner and Fitter efficiencies for the offline IDSCAN version (1000 low luminosity events, 200 high luminosity events)

Distributions for the variables  $P_T$ ,  $\phi - \phi_{true}$ ,  $\eta - \eta_{true}$ ,  $z_0 - z_{0true}$  and  $d_0$  are shown in Figure 2.3 for 20GeV electrons at low luminosity. The  $P_T$  distribution for IDSCAN has a peak at lower  $P_T$  than for xKalman and it also has more events in the tail at high  $P_T$ . These are the same features observed in the muon plots. The distributions for  $\eta - \eta_{true}$ ,  $\phi - \phi_{true}$  and  $z_0 - z_{0true}$  have slightly worse resolutions than xKalman. Notably xKalman has very few events with positive values of  $d_0$  IDSCAN does not have this bias.

The online version of IDSCAN has been performing very badly up until the beginning of June, only reconstructing tracks in about 15% of events. With the reasonable performance of the ATHENA version, it was felt that problems in the online space-points were the most likely cause. The other LVL2 tracking algorithm SiTrack was also performing badly, but they managed to improve their efficiency from 15% to around 60% by resolving problems within their algorithm.

Figure 2.4 shows an ATLANTIS display of the online space-points overlaid onto the track reconstructed by the offline version. On this plot the lowest three hits are

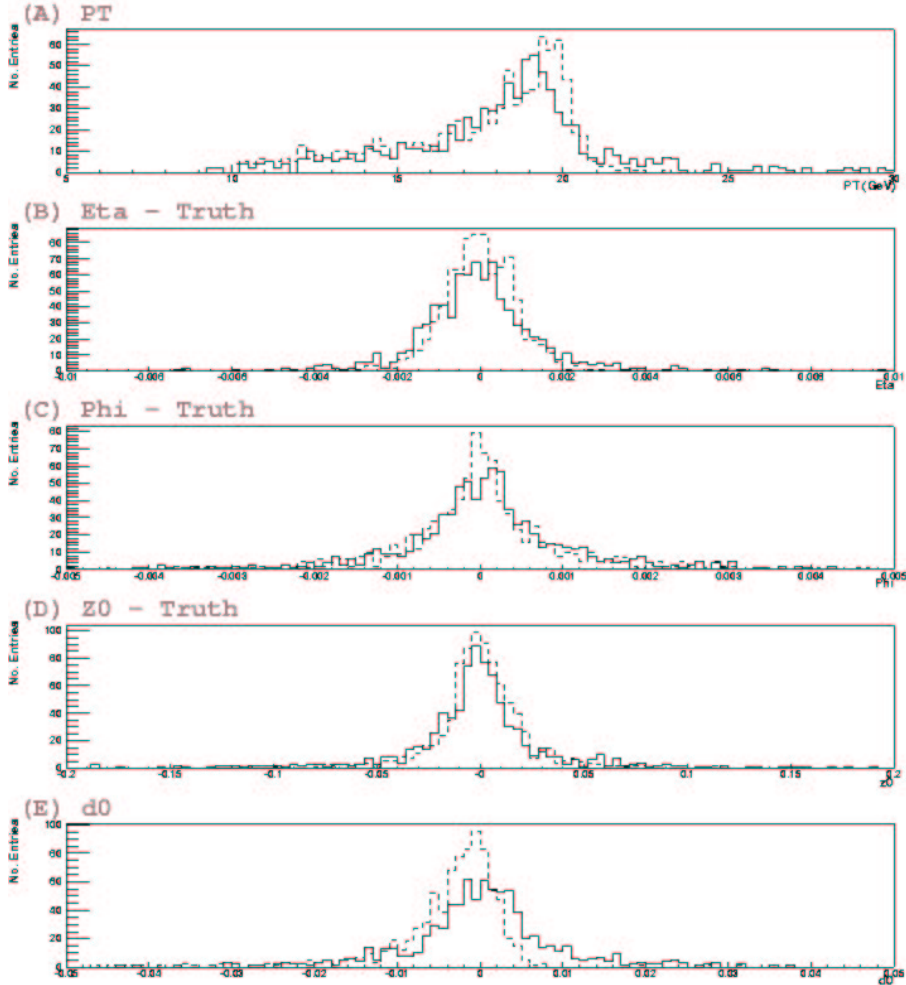


Figure 2.3: Offline (solid-line) and xKKalman(dashed-line) distributions for  $P_T$ ,  $\phi - \phi_{true}$ ,  $\eta - \eta_{true}$ ,  $z_0 - z_{0true}$  and  $d_0$  for 20GeV electrons at low luminosity.

from the Pixel detector and fit the track very well. It is clear that problems are present in the SCT space-points. SiTrack relies heavily on the Pixel space-points making little use of the SCT. This accounts for their improved efficiency.

Issues with the online space-points are being slowly resolved. The latest validation results are summarised in Table 2.3, obtained from 2500 low/high luminosity events and 1000 events without pile-up using the same track selection and efficiency calculation described above.

	20GeV Electron		30GeV Electron	
	No Pile-Up	Low Luminosity	No Pile-Up	High Luminosity
Online	95.7%	90.3%	96.4%	83.3%
Offline	95.4%	95.6%	95.2%	93.3%

Table 2.3: IDSCAN Efficiencies for offline and online versions

The drop in efficiency at high luminosity for the online algorithm is still under investigation. The previous results for the HitFilter performance suggest that this is likely to be due to the ZFinder. The online version has a modified version of



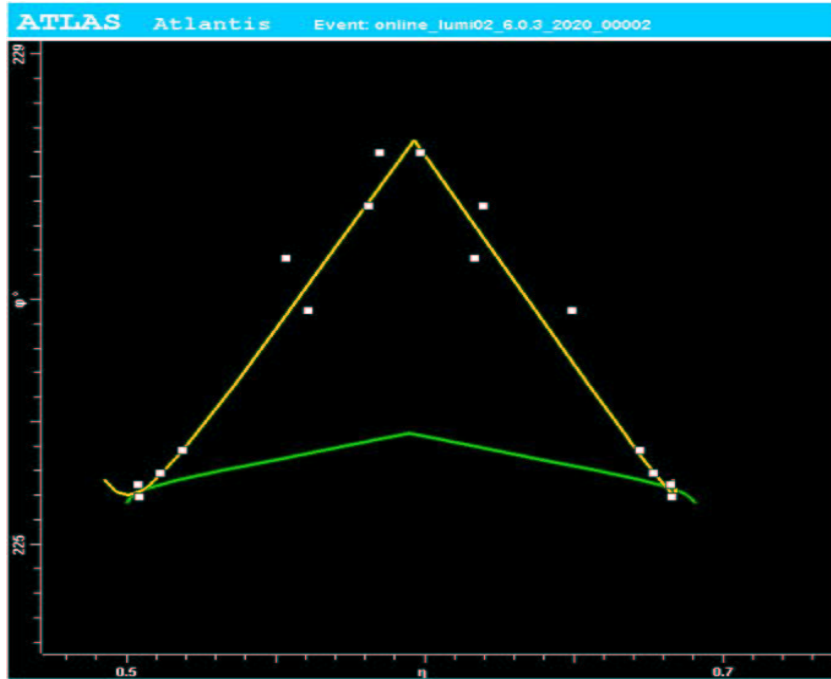


Figure 2.4: An Atlantis V-plot showing the online space-points (white), the track reconstructed by the offline version of IDSCAN (yellow) and the truth track (green). This is an event where the electron has radiated a very energetic photon. A track is a straight line in an  $\phi$ ,  $\eta$  projection. On a V-plot each space-point is drawn twice. The distance between the two in  $\eta$  depends on how far the space-point is from the exit of SCT. Space-points from the Pixel Layers are transformed to be the furthest apart and the last layer of the SCT the closest, giving a V-shape to the track. The charge of the track is given by the way the V points. In this case it points upwards (negative) and the angle of the V gives the momentum. The green track is of high momentum, whereas the yellow reconstructed track, which has radiated an energetic photon, is of low momentum.

the ZFinder, unlike the offline version which has an almost identical version to that in CTRIG. Reverting back to the non-modified version could solve some of the performance issues. However, even for the offline there is some reduction in the performance at high luminosity.

Plots for the  $P_T$ ,  $\eta$ ,  $\phi$ ,  $Z_0$  and  $d_0$  distributions for high luminosity are presented in Figure 2.5. These highlight problems with the  $\eta$  and  $Z_0$  resolutions at high luminosity for the online version. For  $z_0$  the xKalman resolution is  $140\mu\text{m}$  and the offline IDSCAN resolution is  $153\mu\text{m}$ <sup>2</sup>. However, for the online version this has dropped to  $195\mu\text{m}$ . A few problems with the online space-points still remain and could be causing these issues.

<sup>2</sup>This is the z-resolution from the Fitter, not the ZFinder.

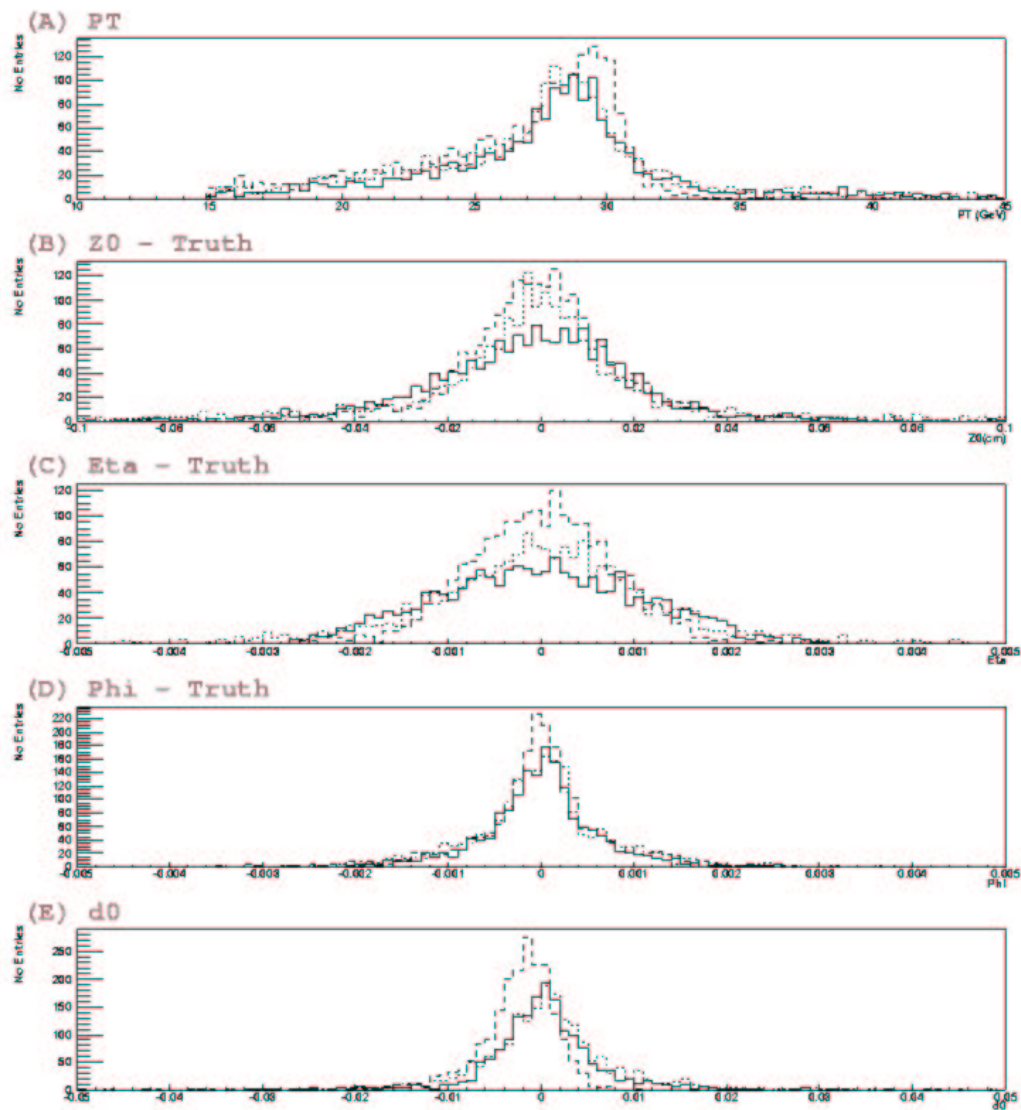


Figure 2.5: Online (solid-line), offline (dotted-line) and xKalman(dashed-line) distributions for  $P_T$ ,  $\phi - \phi_{true}$ ,  $\eta - \eta_{true}$ ,  $z_0 - z_{0true}$  and  $d_0$  for 30GeV electrons at high luminosity.

## 3. Future Plans

Work during the next year will be based around three main areas. These are IDSCAN, ATLANTIS and a physics study of the channel  $t\bar{t}H$ ,  $H \rightarrow b\bar{b}$ , described in turn below.

### 3.1 IDSCAN

The data production for the TDR began a few weeks ago using the offline version of IDSCAN. In the near future IDSCAN is going to be re-implemented and fully tested, hopefully equalling or bettering the performance seen running in CTRIG. The HLT algorithm community aims to submit an ATLAS note around November when all problems with the online trigger chain have been fixed. This will include results from the online version of IDSCAN.

### 3.2 Atlantis

Atlantis is an event display for ATLAS written in Java. It is based on the ALEPH event display DALI. UCL will be taking an increasing role in the development of Atlantis in the future and, in the next few weeks, I shall be meeting with the main developer Gary Taylor to learn about the program.

### 3.3 Associated Higgs Production: $t\bar{t}H$

The channel  $t\bar{t}H$ ,  $H \rightarrow b\bar{b}$  is expected to provide half the significance for the discovery of a standard model Higgs Boson, for the mass range below  $2 m_W$ . Here, the  $H \rightarrow b\bar{b}$  decay mode is dominant with a branching ratio of 90%. However, direct production  $g\bar{g} \rightarrow H$  cannot be efficiently triggered nor extracted due to the huge QCD 2-jet background.

For associated production with a  $W$  or  $t\bar{t}$  pair, the leptonic decay of the  $W$ , or semi-leptonic decay of a top, provides an isolated high  $P_T$  lepton for triggering. In addition the high  $P_T$  lepton provides a large rejection against the QCD jet background.

The  $t\bar{t}H$ ,  $H \rightarrow b\bar{b}$  final state is complex, with four b-jets. Two from the top quark decays and two from the Higgs Boson decay. Two  $W$  bosons are also produced in the top quark decays. One of these is required to decay leptonically and the other to  $q\bar{q}$ , producing a further two jets. Feynman diagrams for these processes are shown in Figure 3.1.

Irreducible backgrounds to these processes include resonant  $t\bar{t}Z$  and continuum  $t\bar{t}b\bar{b}$  production. Since the  $t\bar{t}Z$  cross-section is much smaller than the signal cross-section, the resonant background is not a problem in this channel. Reducible backgrounds include jets misidentified as b-jets, such as  $t\bar{t}jj$ ,  $Wjjjjj$ ,  $WWb\bar{b}jj$  etc. The  $Wjjjjj$  and  $WWb\bar{b}jj$  backgrounds are suppressed to a large extent by the reconstruction of both top decays.

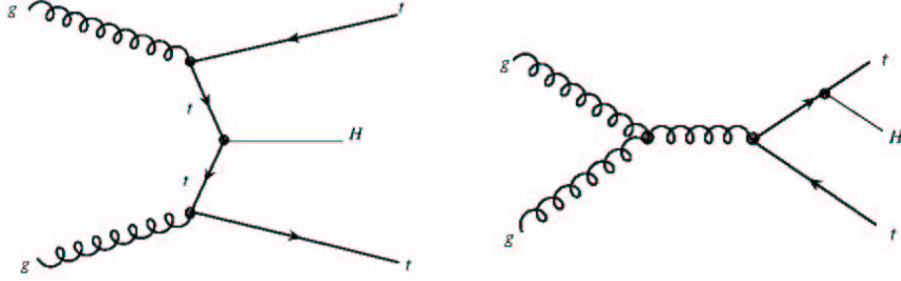


Figure 3.1: Example Feynman Diagrams for  $t\bar{t}H$  production

The analysis procedure used for the physics TDR is described below [ATL99, RW99, Sap01]. Firstly events are selected using the following criteria:

- **One Trigger Lepton**  
With  $P_T > 20\text{GeV}$  (electron) or  $P_T > 6\text{GeV}$  (muon) within  $|\eta| < 2.5$ . At high luminosity these are raised to  $30\text{GeV}$  and  $20\text{GeV}$  respectively.
- **At least six Jets  $> 15\text{GeV}$**   
This is raised to  $30\text{GeV}$  at high luminosity.
- **Exactly four jets tagged as b-jets**

The total acceptance of this selection for inclusive  $t\bar{t}$  events with one  $W \rightarrow l\nu$  is about 33%. For signal events the acceptance is 5.3%.

Both top quarks are reconstructed simultaneously, finding the combination which minimises equation 3.1.

$$\chi^2 = (m_{l\nu b} - m_t)^2 + (m_{jjb} - m_t)^2 \quad (3.1)$$

For the  $W \rightarrow jj$  reconstruction, to minimise the combinatorial background from jets originating from initial or final state QCD radiation, only jets with  $p_T^{jet} > 20\text{GeV}$  are considered. Only  $jj$  combinations with  $m_{jj} = m_W \pm 25\text{GeV}$  ( $\pm 2\sigma_m$  mass window) are retained for further analysis.

Complete reconstruction of  $W \rightarrow l\nu$  is limited by the impossibility of fully reconstructing the neutrino four-momentum. The transverse components of the neutrino momentum are assumed to equal the corresponding components of the missing energy in the event, while the information on the longitudinal component is lost because of the large amount of energy escaping down the beam-pipe. This information can be recovered by solving equation 3.2 for the mass of the W-Boson.

$$m_W^2 = (E^\nu + E^l)^2 - (p_x^\nu + p_x^l)^2 - (p_y^\nu + p_y^l)^2 - (p_z^\nu + p_z^l)^2 \quad (3.2)$$

Here  $p_x^\nu = p_x^{miss}$ ,  $p_y^\nu = p_y^{miss}$  and the neutrino is assumed massless. For the cases where there are no solutions to equation 3.2 the event is rejected. Around 90% of events satisfy this criteria. However comparisons with truth data found only 36% of events have good  $p_z^\nu$  reconstruction, indicated by  $|p_z^\nu - p_z^{\nu-rec}| < 3\sigma$ .

To further reject wrongly reconstructed top decays, only events where both reconstructed top masses lie within  $\pm 20\text{GeV}$  of the nominal top mass are kept. This keeps 66% of reconstructed top decays. Multiplying this with the acceptance of kinematic cuts and lepton and b-tagging efficiencies gives a total acceptance of 1.7% for events

Integrated Luminosity	30fb <sup>-1</sup>			100fb <sup>-1</sup>		
Higgs mass (GeV)	80	100	120	80	100	120
Signal S	81	61	40	140	107	62
$t\bar{t}Z$	7	8	2	13	13	5
$Wjjjjjj$	17	12	5	35	15	10
$t\bar{t}jj$	121	130	120	247	250	242
Total Background B	145	150	127	295	278	257
S/B	0.56	0.41	0.32	0.47	0.38	0.24
$S/\sqrt{B}$	6.7	5.0	3.6	8.2	6.4	3.9
$S_{H\rightarrow b\bar{b}}/S_{total}$	0.67	0.64	0.59	0.57	0.53	0.50

Table 3.1: Expected  $t\bar{t}H$  signal and background rates for three different Higgs-Boson masses [ATL99].

at low luminosity. At high luminosity the  $P_T$  thresholds for the lepton and jets are raised to 30GeV and the b-tagging efficiencies are reduced from 60% to 50%, giving an acceptance of 0.7%.

For the Higgs reconstruction, the mass window cut is  $\pm 30\text{GeV}$  and has an efficiency of 41% for signal events. For 64% of events in this mass window the jet assignment is correct. At high luminosity the window is increased to  $\pm 45\text{GeV}$ , due to a decrease in the mass resolution, resulting in an acceptance of 50% and correct jet assignment of 50%. Table 3.3 summarises the signal and background event numbers and the expected significance of the channel at the time of the TDR.

Work carried out since the TDR in 1999 has re-estimated these significances with the CTEQ5L parton density functions, a QCD scale of  $Q_{QCD}^2 = (m_t + m_H/2)^2$  instead of PYTHIA default<sup>1</sup> as well as updated signal cross sections, branching ratios and irreducible backgrounds. This was found to reduce the significance of this channel for  $m_H=100\text{GeV}$  from 5.0 to 3.6 and for  $m_H=120\text{GeV}$  from 3.6 to 1.9 at low luminosity.

Further improvements to the analysis have include a collinear approximation ( $p_\nu^z = p_i^z$ ), for events where equation 3.2 cannot be solved, and pairing likelihoods used for top and Higgs reconstruction instead of mass cuts. These studies have quoted a 40% overall gain in the significance in comparison to their updated studies using the TDR analysis method [Cam03].

The  $t\bar{t}H \rightarrow b\bar{b}$  channel relies heavily on excellent b-tagging efficiencies. The reduction of signal events due to the requirement of four b-tagged jets is 91.9%. There are currently no b-tagging algorithms for ATLAS and tagging is done randomly on true b-jets, with an efficiency of 60% for low luminosity and 50% for high luminosity. Realistic b-tagging would be one way to improve this analysis.

The knowledge of the large  $t\bar{t}jj$  background is another area where substantial improvement could be made. The cross section for  $t\bar{t}$ +jets is 500pb compared to 0.52pb for  $t\bar{t}H$  ( $m_H=120\text{GeV}$  Higgs). After analysis, this background constitutes 94% of the total background. Full understanding could lead to possible improvements to the analysis and significance of this channel.

<sup>1</sup>The PYTHIA default depends on the process



# Bibliography

- [ATL94] ATLAS. Atlas technical proposal. Technical report, 15 December 1994.
- [ATL99] ATLAS. Atlas detector and physics report, technical design report. Technical report, 25 May 1999.
- [ATL03a] ATLAS. Algorithms for the atlas high level trigger. Technical report, 10 June 2003.
- [ATL03b] ATLAS. High-level triggers, daq and dcs - technical design report. Technical report, 30 June 2003.
- [Cam03] Jochen Cammin. The atlas discovery potential for the channel  $t\bar{t}h$ ,  $h \rightarrow b\bar{b}$ . June 2003.
- [Gro03a] PESA Core Algorithms Group. Algorithms for the atlas high level trigger. ATLAS-DAQ-2003-013, June 2003.
- [Gro03b] PESA Core Algorithms Group. An overview of algorithms for the atlas high level trigger. ATLAS-CONF-2003-003, June 17 2003.
- [NK00] H. Drevermann N. Konstantinidis. Fast tracking in hadron collider experiments. *ACAT2000 Conference Proceedings*, page 130, October 2000.
- [RW99] Elzbieta Richter-Was. Search for the sm and mssm higgs boson in the  $t\bar{t}h$ ,  $h \rightarrow b\bar{b}$  channel. *ACTA PHYSICA POLONICA B*, 30(4):1001–1040, 1999.
- [Sap01] Mariusz Sapinski. *Search for the Higgs Boson in multi-jet final states with ATLAS detector at LHC*. PhD thesis, Academy of Mining and Metallurgy, Krakow, May 2001.